

Spatial entanglement in two-electron atomic systems

Yen-Chang Lin, Chih-Yuan Lin,^{*} and Yew Kam Ho[†]*Institute of Atomic and Molecular Sciences, Academia Sinica, P.O. Box 23-166, Taipei 106, Taiwan*

(Received 29 June 2012; published 13 February 2013)

Recently, there has been considerable interest in investigating quantum entanglement in two-electron systems, such as two-electron model atoms and quantum dots. In this work, the quantum entanglement of the helium atom and helium-like ions are explored using the two-electron wave functions constructed by the B -spline basis. As a measure of the spatial entanglement, the linear entropy of the reduced density matrix is investigated for the ground state and the singlet excited $1sns^1S$ states, with $n = 2-10$, of the helium atom. The variation of the spatial entanglement with the nuclear charges $Z = 2-15$ for the helium-like ions is reported. Results are compared with the existing predictions.

DOI: [10.1103/PhysRevA.87.022316](https://doi.org/10.1103/PhysRevA.87.022316)

PACS number(s): 03.67.Bg, 03.65.Ud, 31.15.ve

I. INTRODUCTION

As one of the most essential characteristics of the quantum world, quantum entanglement, depicting the inseparable links of composite quantum systems, plays a crucial role for understanding a variety of physical phenomena, such as quantum correlations, phase transitions [1], and chaotic properties [2]. Besides the interest of conceptual development in quantum physics, the entanglement also provides possible technological applications in quantum information, quantum computing [3], quantum cryptography [4], and quantum teleportation [5].

Recently, a great deal of effort has been made to investigate the role of entanglement in atomic systems, including two-electron model atoms, helium-like ions, and helium atoms. The review article by Tichy *et al.* [6] has given a detailed discussion on essential entanglement for atomic and molecular systems. For the model atoms, the Moshinsky atom [7], which is characterized by the harmonic confining potential and the harmonic electron-electron interaction, has been widely investigated in previous studies [8–12]. The Crandall and the Hooke atoms are two alternative model atoms which have attracted much attention recently [13–15]. Both model atoms have the harmonic confining potential, but the Crandall atom has an inverse cubic electron-electron repulsion force, while the Hooke atom has the Coulomb electron-electron interaction. Being an artificial atom, the quantum dot has been analyzed for the spatial entanglement between two trapped electrons [16].

Based on the previous work for the two-electron model atoms, the trends of entanglement measures varying with the state energies and the nuclear charges have been observed and reported [17]. However, the research efforts made on real two-electron atoms, i.e., the helium atom [18] and helium-like ions [13,14], are relatively sparse. It is interesting to uncover the resemblance and different properties of the entanglement for the real two-electron atoms. The present work proposes an alternative computing approach to explore the spatial entanglement of the helium atom and helium-like ions. In Sec. II, the linear entropy as a spatial entanglement measure is introduced, and the method of the B -spline configuration interaction is briefly described. In Sec. III, the results for

the helium atom and helium-like ions for the ground and excited states are presented and discussed. Comparisons are made to existing results. Section IV summarizes this work and gives conclusions. Atomic units are used throughout unless otherwise noted.

II. THEORETICAL METHOD

The entanglement of atomic systems is quantified using different entanglement entropies, such as von Neumann and linear entropies. In this work, we focus on the linear entropy, which is an approximation of von Neumann entropy:

$$S(\rho) = -\text{Tr}(\rho \ln \rho), \quad (1)$$

where ρ is the density matrix. The natural logarithm can be expanded as

$$\ln \rho = (\rho - 1) - \frac{(\rho - 1)^2}{2} + \frac{(\rho - 1)^3}{3} + \dots \quad (2)$$

We can rewrite the von Neumann entropy as

$$\begin{aligned} & -\text{Tr}(\rho \ln \rho) \\ &= -\text{Tr} \left[\rho(\rho - 1) - \frac{\rho(\rho - 1)^2}{2} + \frac{\rho(\rho - 1)^3}{3} + \dots \right]. \end{aligned} \quad (3)$$

The leading term gives linear entropy. In the present work, it is defined as $L_s = 1 - \text{Tr} \rho_{\text{red}}^2$, where ρ_{red} is the reduced density matrix. For two-component quantum systems, e.g., two-electron atoms, the reduced density matrix ρ_{red} is obtained by tracing the two-particle density matrix over one of the two particles.

The state wave functions of two-electron systems can be described by

$$\Phi = \Psi \chi, \quad (4)$$

where the spatial and spin components Ψ and χ , respectively, are factorized. In this work, we concentrate on the singlet-spin states with antiparallel spins, which lead to a constant value of $1/2$ for tracing the spin part of the reduced density matrix. Therefore, the entanglement of two-electron atoms is well characterized by the spatial degree of freedom of the reduced density matrix,

$$\rho_{\text{red}}(\mathbf{r}_1, \mathbf{r}_2) = \int \Psi^*(\mathbf{r}_1, \mathbf{r}_3) \Psi(\mathbf{r}_2, \mathbf{r}_3) d\mathbf{r}_3. \quad (5)$$

^{*}cylin@pub.iams.sinica.edu.tw
[†]ykho@pub.iams.sinica.edu.tw

As given by Coe *et al.* [15], the square of the reduced density matrix is

$$\rho_{\text{red}}^2(\mathbf{r}_1, \mathbf{r}_2) = \int \rho_{\text{red}}(\mathbf{r}_1, \mathbf{r}_3) \rho_{\text{red}}(\mathbf{r}_3, \mathbf{r}_2) d\mathbf{r}_3, \quad (6)$$

and

$$\text{Tr} \rho_{\text{red}}^2 = \int \rho_{\text{red}}^2(\mathbf{r}, \mathbf{r}) d\mathbf{r}. \quad (7)$$

For two-electron atoms, the basis function $\psi_{nl, n'l'}^\Lambda(\mathbf{r}_1, \mathbf{r}_2)$, with Λ standing for a set of quantum number (S, L, M_S, M_L) , can be constructed through the expansion of two-particle Slater-determinant wave functions [19], i.e.,

$$\begin{aligned} \psi_{nl, n'l'}^\Lambda(\mathbf{r}_1, \mathbf{r}_2) &= \sum_{mm', m_s, m'_s} (-1)^{l'-l} [(2S+1)(2L+1)]^{1/2} \\ &\times \begin{pmatrix} l & l' & L \\ m & m' & -M_L \end{pmatrix} \begin{pmatrix} \frac{1}{2} & \frac{1}{2} & S \\ m_s & m'_s & -M_S \end{pmatrix} \\ &\times \phi_{nl, n'l'}^{mm', m_s, m'_s}(\mathbf{r}_1, \mathbf{r}_2). \end{aligned} \quad (8)$$

where the Slater-determinant wave function $\phi_{nl, n'l'}^{mm', m_s, m'_s}(\mathbf{r}_1, \mathbf{r}_2)$ is given by the one-particle orbital $u_{nl}^{mm_s}$ including spin, i.e.,

$$\begin{aligned} \phi_{nl, n'l'}^{mm', m_s, m'_s}(\mathbf{r}_1, \mathbf{r}_2) \\ = \frac{1}{\sqrt{2}} [u_{nl}^{mm_s}(\mathbf{r}_1) u_{n'l'}^{m'_s}(\mathbf{r}_2) - u_{nl}^{mm_s}(\mathbf{r}_2) u_{n'l'}^{m'_s}(\mathbf{r}_1)]. \end{aligned} \quad (9)$$

It is worth mentioning that a factor of $1/\sqrt{2}$ should be added to Eq. (8) for the normalization as $nl = n'l'$.

The radial function $\chi_{nl}(r)$ of the one-particle orbital is expanded in terms of the B -spline basis functions $B_{i,k}(r)$, i.e.,

$$\chi_{nl}(r) = \sum_{i=1}^N C_i B_{i,k}(r). \quad (10)$$

Along the r axis with end points $r = 0$ and $r = R$, we select a knot sequence $\{t_i\}$ ($i = 1, 2, 3, \dots, N+k$), in which $t_i \leq t_{i+1}$. The B -spline basis functions of order k are defined on the knot sequence by the following recurrence relations [20]:

$$B_{i,1}(r) = \begin{cases} 1 & \text{for } t_i \leq r < t_{i+1}, \\ 0 & \text{otherwise} \end{cases} \quad (11)$$

and

$$B_{i,k}(r) = \frac{r - t_i}{t_{i+k-1} - t_i} B_{i,k-1}(r) + \frac{t_{i+k} - r}{t_{i+k} - t_{i+1}} B_{i+1,k-1}(r). \quad (12)$$

The boundary conditions of the radial wave functions require $\phi(0) = \phi(R) = 0$, which leads to the vanished coefficients C_1 and C_N because of the properties of the B splines at two end points, i.e., $B_{1,k}(0) = 1$ and $B_{N,k}(R) = 1$.

Within the framework of the configuration interaction method, we had implemented the finite basis approach using the B -spline basis functions to obtain the high-quality wave functions of the helium atom [21]. In the present work, the one-electron basis functions including s , p , d , f , g , and h orbitals with the principal quantum number n up to 40 are used to construct two-electron wave functions for ~ 4000 1S configurations. Through the diagonalization of the Hamiltonian matrix, the eigenvalues and eigenvectors can

be obtained, in which the eigenvectors are essential for the calculation of the linear entropy. Using Eqs. (5)–(7) with the wave functions expanded in terms of the basis functions (8) but not including the spin part, i.e.,

$$\phi_{nl, n'l'}^{mm'}(\mathbf{r}_1, \mathbf{r}_2) = \frac{1}{\sqrt{2}} [u_{nl}^m(\mathbf{r}_1) u_{n'l'}^{m'}(\mathbf{r}_2) + u_{nl}^m(\mathbf{r}_2) u_{n'l'}^{m'}(\mathbf{r}_1)], \quad (13)$$

the trace of the square of reduced density matrix for the singlet S states is given as

$$\begin{aligned} \text{Tr} \rho_{\text{red}}^2 &= \frac{1}{4} \sum_{l, n_1, n_2, n_3, n_4} \{J(l, m) [C_{n_1, n_2}^l C_{n_3, n_2}^l C_{n_1, n_4}^l C_{n_3, n_4}^l \\ &+ C_{n_1, n_2}^l C_{n_3, n_2}^l C_{n_1, n_4}^l C_{n_4, n_3}^l \\ &+ C_{n_1, n_2}^l C_{n_2, n_3}^l C_{n_1, n_4}^l C_{n_3, n_4}^l + C_{n_1, n_2}^l C_{n_2, n_3}^l C_{n_1, n_4}^l C_{n_4, n_3}^l \\ &+ C_{n_1, n_2}^l C_{n_3, n_1}^l C_{n_4, n_2}^l C_{n_3, n_4}^l + C_{n_1, n_2}^l C_{n_3, n_1}^l C_{n_4, n_2}^l C_{n_4, n_3}^l \\ &+ C_{n_1, n_2}^l C_{n_1, n_3}^l C_{n_4, n_1}^l C_{n_3, n_4}^l + C_{n_1, n_2}^l C_{n_1, n_3}^l C_{n_4, n_2}^l C_{n_4, n_3}^l] \\ &+ J(l, 0) [C_{n_1, n_2}^l C_{n_3, n_1}^l C_{n_2, n_4}^l C_{n_3, n_4}^l \\ &+ C_{n_1, n_2}^l C_{n_3, n_1}^l C_{n_2, n_4}^l C_{n_4, n_3}^l + C_{n_1, n_2}^l C_{n_1, n_3}^l C_{n_2, n_4}^l C_{n_3, n_4}^l \\ &+ C_{n_1, n_2}^l C_{n_1, n_3}^l C_{n_2, n_4}^l C_{n_4, n_3}^l + C_{n_1, n_2}^l C_{n_3, n_2}^l C_{n_4, n_1}^l C_{n_3, n_4}^l \\ &+ C_{n_1, n_2}^l C_{n_3, n_2}^l C_{n_4, n_1}^l C_{n_4, n_3}^l + C_{n_1, n_2}^l C_{n_2, n_3}^l C_{n_4, n_1}^l C_{n_3, n_4}^l \\ &+ C_{n_1, n_2}^l C_{n_2, n_3}^l C_{n_4, n_1}^l C_{n_4, n_3}^l]\}, \end{aligned} \quad (14)$$

where C_{n_a, n_b}^l is a component of the eigenvector corresponding to a configuration (n_a, l_a, n_b, l_b) with $n_a \leq n_b$ and $l_a = l_b = l$. For the present case with total angular momentum $L = 0$, the orbital angular momenta of each electron, l_a and l_b , must be equal. The factor $J(l, m)$ is defined as

$$J(l, m) = \sum_m \begin{pmatrix} l & l & 0 \\ m & -m & 0 \end{pmatrix}^4 \quad (15)$$

and

$$J(l, 0) = \begin{pmatrix} l & l & 0 \\ 0 & 0 & 0 \end{pmatrix}^4. \quad (16)$$

It should be noted that an additional factor of $\frac{1}{4}$ needs to be added to Eq. (14) for $n_a = n_b$.

III. RESULTS AND DISCUSSION

To explore the entanglement features of real atomic systems instead of the atomic models, we perform calculations of linear entropy as a measure of the spatial entanglement for the helium atom and helium-like ions. For the helium atom, Coe and D'Amico [14] studied the variation of spatial entanglement with the strength of the electron-nucleus interaction using the local-density approximation. They also calculated the linear entropy for the ground state of the helium atom with wave functions constructed by using the products of hydrogenic wave functions [14]. Manzano *et al.* [13] also investigated the entanglement of the helium ground and excited states using the Kinoshita-type wave functions. Recently, the same approach facilitated by the Monte Carlo multidimensional integration was implemented by Dehesa *et al.* [18] to explore the $1s n s$ 1S and 3S states of the helium atom for n up to 5. Our calculation of the helium ground state carried out by the

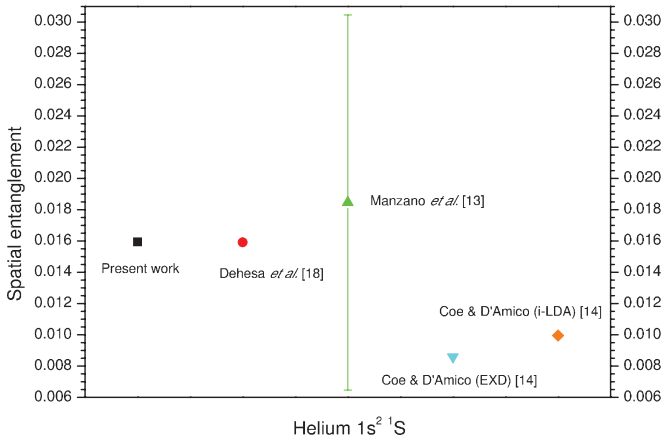


FIG. 1. (Color online) Spatial entanglement of helium ground state. i-LDA: interacting local-density approximation; EXD: exact diagonalization with a basis constructed using products of hydrogenic wave functions [14].

B-spline configuration interaction method for linear entropy as a measure of the spatial entanglement is presented in Fig. 1 and compared to existing results. The present calculation is in good agreement with the prediction by Dehesa *et al.* [18]. The data reported by Coe and D'Amico [14] show a smaller amount of entanglement. It should be noted that the result of Manzano *et al.* [13] involves large variances due to the Monte Carlo calculations. For the prediction by Dehesa *et al.* [18], the variances are significantly reduced.

In Fig. 2, we demonstrate the linear entropy for the helium $1sns\ ^1S$ states with n up to 10. The linear entropy, which tends to reach a saturated value with increasing the quantum number n , i.e., increasing the state energy, has been observed in several model atoms, such as the Crandall, Hooke, and Moshinsky models. This trend is also exhibited by the real helium atom, but with a saturated value of 0.5 instead of 1 due to the Coulomb potential [18]. Our results shown in Fig. 2 present a relatively stable trend compared to the data reported by Dehesa *et al.* [18]. In our present work, by using different expansion terms in the wave functions, we have estimated the uncertainty of the linear entropy for the ground $1s^2\ ^1S^e$ state of He is about ± 0.000040 . For excited $1sns$ states, with $2 \leq n \leq 5$ and with $6 \leq n \leq 10$ the estimated uncertainties are ± 0.00020 and ± 0.00010 , respectively. It is

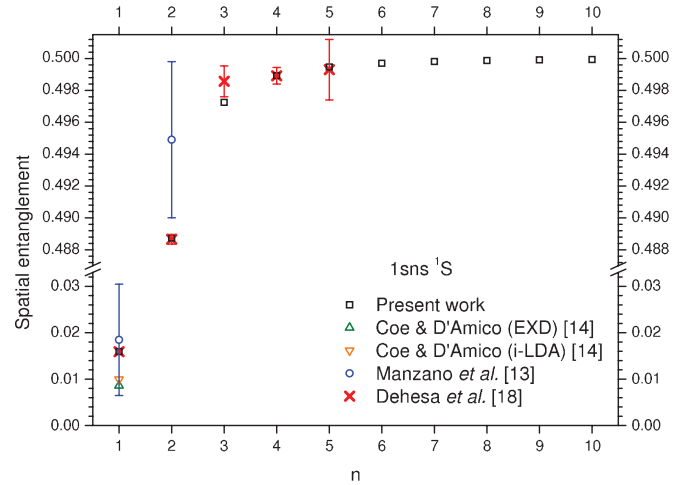


FIG. 2. (Color online) Variation of the spatial entanglement with the helium states of $1sns\ ^1S$ ($n = 1-10$). i-LDA: interacting local-density approximation; EXD: exact diagonalization with a basis constructed using products of hydrogenic wave functions [14].

seen that our results agree with those of Dehesa *et al.* [18] quite well, except for the $1s3s\ ^1S$ state, which lies slightly outside our combined estimated uncertainties. Using the present computation scheme, we can perform calculations for higher excited states with less computational cost. The linear entropy approaching the saturated value of 0.5 is clearly illustrated.

For highly excited states, i.e., $1sns\ ^1S$ with large n , the electron-electron interaction is relatively small compared to the electron-nucleus interaction. One configuration constructed by employing the $1s$ and ns hydrogenic wave functions can properly describe the state. Based on this approximation, the linear entropy equal to 0.5 is obtained. As n decreases, the interactions between electrons are increased, so that the configuration interactions should be taken into account, which leads to a decrease of spatial entanglement from 0.5. On the other hand, for the ground state, spatial entanglement equal to zero can be obtained as one Slater determinant of two $1s$ orbitals is implemented. Due to the strong correlation between two $1s$ electrons, more configurations are needed for the ground state, which results in the deviation of spatial entanglement from zero.

The values for linear entropy varying with the energies of singlet helium states is listed in Table I. The present energies

TABLE I. Energies and linear entropies of helium atom for the singlet *S* states.

State	Energy (in atomic units)			Linear entropy	
	This work	Dehesa <i>et al.</i> [18]	Drake [22]	This work	Dehesa <i>et al.</i> [18]
$1s^2\ ^1S$	-2.9035869	-2.903724377	-2.9037243770341195	0.015943	0.015914 ± 0.000044
$1s2s\ ^1S$	-2.1459653	-2.145974046	-2.145974046054419	0.488736	0.48866 ± 0.00030
$1s3s\ ^1S$	-2.0612695	-2.061271954	-2.061271989740911	0.497251	0.49857 ± 0.00097
$1s4s\ ^1S$	-2.0335856	-2.033586653	-2.03358671703072	0.498925	0.49892 ± 0.00052
$1s5s\ ^1S$	-2.0211762	-2.021176531	-2.021176851574363	0.499471	0.4993 ± 0.0019
$1s6s\ ^1S$	-2.0145627		-2.01456309844660	0.499701	
$1s7s\ ^1S$	-2.0106255		-2.01062577621087	0.499815	
$1s8s\ ^1S$	-2.0080934		-2.00809362210561	0.499877	
$1s9s\ ^1S$	-2.0063693		-2.00636955310785	0.499915	
$1s10s\ ^1S$	-2.0051391		-2.00514299174800	0.499937	

TABLE II. Linear entropies of $1sns^1S$ ($n = 1-10$) states for the two-electron atoms with $Z = 3-15$.

	Linear entropy												
	$Z = 3$	$Z = 4$	$Z = 5$	$Z = 6$	$Z = 7$	$Z = 8$	$Z = 9$	$Z = 10$	$Z = 11$	$Z = 12$	$Z = 13$	$Z = 14$	$Z = 15$
$1s^2\ ^1S$	0.006549	0.003562	0.002237	0.001535	0.001118	0.000851	0.000669	0.000539	0.000444	0.000372	0.000316	0.000272	0.000236
$1s2s\ ^1S$	0.493030	0.495637	0.497070	0.497912	0.498442	0.498795	0.499041	0.499219	0.499352	0.499454	0.499534	0.499597	0.499649
$1s3s\ ^1S$	0.498382	0.499035	0.499376	0.499568	0.499684	0.499760	0.499812	0.499849	0.499876	0.499896	0.499912	0.499925	0.499935
$1s4s\ ^1S$	0.499379	0.499637	0.499769	0.499842	0.499886	0.499914	0.499933	0.499946	0.499956	0.499964	0.499969	0.499974	0.499977
$1s5s\ ^1S$	0.499696	0.499824	0.499889	0.499925	0.499946	0.499959	0.499968	0.499975	0.499980	0.499983	0.499986	0.499988	0.499989
$1s6s\ ^1S$	0.499829	0.499901	0.499938	0.499958	0.499970	0.499978	0.499983	0.499986	0.499989	0.499991	0.499992	0.499993	0.499994
$1s7s\ ^1S$	0.499894	0.499939	0.499962	0.499974	0.499982	0.499986	0.499989	0.499992	0.499993	0.499994	0.499995	0.499996	0.499996
$1s8s\ ^1S$	0.499930	0.499960	0.499975	0.499983	0.499988	0.499991	0.499993	0.499994	0.499995	0.499996	0.499997	0.499997	0.499998
$1s9s\ ^1S$	0.499951	0.499972	0.499983	0.499988	0.499992	0.499994	0.499995	0.499996	0.499997	0.499997	0.499998	0.499998	0.499998
$1s10s\ ^1S$	0.499965	0.499980	0.499987	0.499991	0.499994	0.499996	0.499996	0.499997	0.499998	0.499998	0.499998	0.499998	0.499999

agree reasonably well with the most accurate results predicted by Drake [22] from the $1s^2\ ^1S$ to $1s10s\ ^1S$ state, and the agreement gets better for the higher excited states. The small value of the linear entropy for the ground helium state indicates the small entanglement for two tightly bound electrons. As one electron is transitioned to the higher excited states and the other one remains tightly bound, the linear entropy rapidly increases. The linear entropies monotonically increasing with the state energies are observed.

For the helium-like atoms, the entanglement of the ground state varying with the nuclear charge from $Z = 2$ to 15 is presented in Fig. 3. Our results are in good agreement with the existing data [13,14] for the ground states showing the

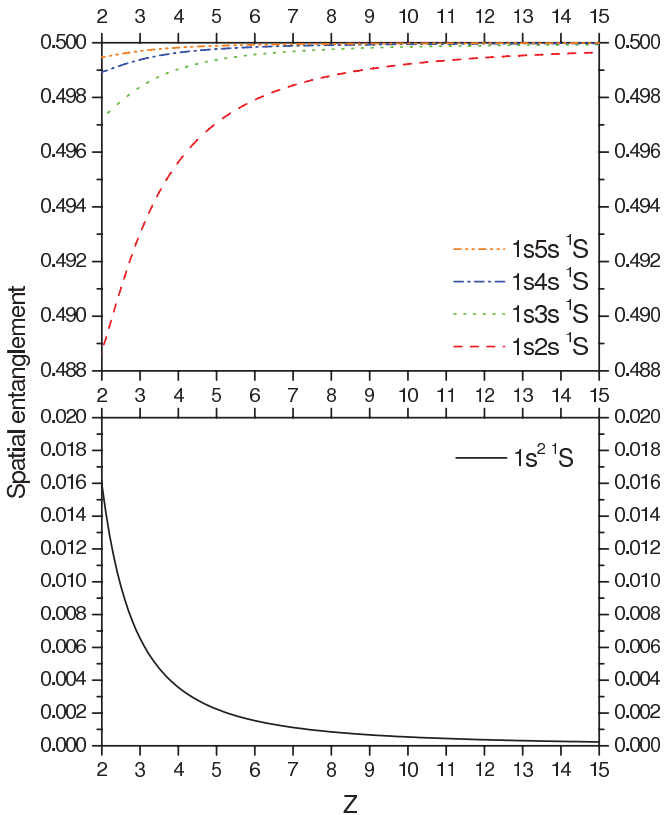


FIG. 3. (Color online) Variation of the spatial entanglement with the nuclear charge Z for the ground and excited states of two-electron atoms.

declining trend of the linear entropy with increasing nuclear charge Z . It is attributed to the decrease of the ratio of electron-electron interaction to the nucleus-electron interaction. When the nucleus-electron attraction potential dominates that of the electron-electron repulsion with increasing Z to a large value, the ground state starts to behave like the product of two hydrogenic ground-state wave functions. An independent particle model can be used to estimate the limiting case for the helium-like ions. Using one configuration, i.e., one single Slater determinant consisting of hydrogenic orbitals to represent the singlet ground state (Hartree-Fock approximation), it is straightforward to find $\text{Tr}\rho_{\text{red}}^2 = 1$, which means the linear entropy is approaching zero. That is the reason why the spatial entanglement approaches zero with increasing Z in Fig. 3. The deviation from zero, such as $\sim 1.1\%$ for $Z = 7$ and $\sim 0.024\%$ for $Z = 15$, indicates the contribution from the configuration interaction effect. Obviously, the configuration interaction plays a crucial role for small- Z cases where the electron-electron interaction is important. In contrast to the ground state, the excited states exhibit a different trend for increasing nuclear charge. As shown in Fig. 3, the linear entropies for the excited states with increasing nuclear charge Z approach 0.5 for large Z . The detailed data for the linear entropy of the excited singlet S states as functions of nuclear charge Z are listed in Table II. Based on the similar hydrogenic model, as Z is increased, the nucleus-electron attractive potential starts to dominate that of the electron-electron repulsion. The excited 1S state for two-electron systems with one electron tightly bound and the other electron highly excited would start to resemble the following:

$$\frac{1}{\sqrt{2}}[\Psi_{1s}(\mathbf{r}_1)\Psi_{ns}(\mathbf{r}_2) + \Psi_{ns}(\mathbf{r}_1)\Psi_{1s}(\mathbf{r}_2)] \times \frac{1}{\sqrt{2}}[(\uparrow)_1(\downarrow)_2 - (\downarrow)_1(\uparrow)_2], \quad (17)$$

with the (\uparrow) and (\downarrow) denoting the spin-up and spin-down wave functions for the electrons, respectively, and where $\Psi_{1s}(\mathbf{r}_1)$ and $\Psi_{ns}(\mathbf{r}_2)$ are the hydrogenic ground state and excited ns state, respectively, of the helium-like ion. The symmetric radial part of the wave function will lead to the limiting case for a linear entropy of 0.5 as Z is further increased. Our present results for linear entropies as shown in Fig. 3 and Table II are consistent with the physics discussed above.

IV. CONCLUSIONS

Based on the configuration interaction approach, we have investigated the spatial entanglement of the helium atom and helium-like ions using the B -spline basis functions. We perform calculations for linear entropy as a measure of the spatial entanglement of two electrons to explore the helium ground state and $1sns\ ^1S$ ($n = 2-10$) excited states. The present computing approach provides the entanglement results for higher excited states (from $n = 6$ to $n = 10$). Our calculations show an increase of linear entropies with increasing quantum number n or with increasing state energies. The saturated value of 0.5 for the linear entropy is clearly

demonstrated as one of the two electrons in the helium atom is about to be ionized. The influence of nuclear charge on the spatial entanglement has also been studied for helium-like ions. For the ground states of helium-like ions, it is observed that the linear entropy increases for decreasing Z from $Z = 15$ down to $Z = 2$. However, the reverse behavior of the spatial entanglement, which is increased with increasing nuclear charge, is observed for the excited states.

ACKNOWLEDGMENT

Financial support from the National Science Council of Taiwan (ROC) is gratefully acknowledged.

-
- [1] O. Osenda and P. Serra, *Phys. Rev. A* **75**, 042331 (2007).
 - [2] S. Chaudhury, A. Smith, B. E. Anderson, S. Ghose, and P. S. Jessen, *Nature (London)* **461**, 768 (2009).
 - [3] M. A. Nielsen and I. L. Chuang, *Quantum Computation and Quantum Information* (Cambridge University Press, Cambridge, 2000).
 - [4] D. S. Naik, C. G. Peterson, A. G. White, A. J. Berglund, and P. G. Kwiat, *Phys. Rev. Lett.* **84**, 4733 (2000).
 - [5] M.-J. Zhao, S.-M. Fei, and X. Li-Jost, *Phys. Rev. A* **85**, 054301 (2012).
 - [6] M. C. Tichy, F. Mintert, and A. Buchleitner, *J. Phys. B* **44**, 192001 (2011).
 - [7] M. Moshinsky, *Am. J. Phys.* **36**, 52 (1968).
 - [8] C. Amovilli and N. H. March, *Phys. Rev. A* **67**, 022509 (2003).
 - [9] C. Amovilli and N. H. March, *Phys. Rev. A* **69**, 054302 (2004).
 - [10] J. Pipek and I. Nagy, *Phys. Rev. A* **79**, 052501 (2009).
 - [11] I. Nagy and J. Pipek, *Phys. Rev. A* **81**, 014501 (2010).
 - [12] R. J. Yañez, A. R. Plastino, and J. S. Dehesa, *Eur. Phys. J. D* **56**, 141 (2010).
 - [13] D. Manzano, A. R. Plastino, J. S. Dehesa, and T. Koga, *J. Phys. A* **43**, 275301 (2010).
 - [14] J. P. Coe and I. D'Amico, *J. Phys. Conf. Ser.* **254**, 012010 (2010).
 - [15] J. P. Coe, A. Sudbery, and I. D'Amico, *Phys. Rev. B* **77**, 205122 (2008).
 - [16] S. Abdullah, J. P. Coe, and I. D'Amico, *Phys. Rev. B* **80**, 235302 (2009).
 - [17] A. P. Majtey, A. R. Plastino, and J. S. Dehesa, *J. Phys. A* **45**, 115309 (2012).
 - [18] J. S. Dehesa, T. Koga, R. J. Yanez, A. R. Plastino, and R. O. Esquivel, *J. Phys. B* **45**, 015504 (2012); **45**, 239501 (2012).
 - [19] T.-N. Chang, *Many-Body Theory of Atomic Structure and Photoionization* (World Scientific, Singapore, 1993).
 - [20] C. de Boor, *A Practical Guide to Splines* (Springer, New York, 2001).
 - [21] Y.-C. Lin, C.-Y. Lin, and Y. K. Ho, *Phys. Rev. A* **85**, 042516 (2012).
 - [22] G. W. F. Drake, *Atomic, Molecular, and Optical Physics Handbook* (AIP Press, New York, 1996), pp. 154–171.